Influence of the pavement surface on the vibrations induced by heavy traffic in road bridges

A. Camara[1], V.F. Vázquez[2], A.M. Ruiz-Teran[3], S.E. Paje[2]

(1) Department of Civil Engineering at City, University of London, Northampton Square, London EC1V 0HB. Email: alfredo.camara@city.ac.uk. Tel.: +44 (0)20 7040 0082

(2) Laboratory of Acoustic Applied to Civil Engineering, University of Castilla-La Mancha, Avda. Camilo José Cela s/n, 13071 Ciudad Real, Spain

(3) Department of Civil and Environmental Engineering. Imperial College London. South Kensington Campus. Exhibition Rd, London SW7 2AZ, United Kingdom.

Cite as:
Camara A, Vazquez VF, Ruiz-Teran AM, Paje SE (2017). Influence of the pavement surface on the vibrations induced by heavy traffic in road bridges. Canadian Journal of Civil Engineering. In press.
Date of acceptance: 27/08/2017

ABSTRACT

The irregularity of the pavement surface governs the traffic-induced vibrations in road bridges, but it is either ignored or simulated by means of ideal pavements that differ significantly from real cases. This work presents a detailed dynamic analysis of a heavy truck crossing a 40-m span composite deck bridge using on-site measurements of different existing road profiles, as well as code-based ideal pavements. By activating or deactivating certain spatial frequency bands of the pavement, it is observed that the ranges 0.2 - 1 and 0.02 - 0.2 cycles/m are critical for the comfort of the pedestrians and the vehicle users, respectively. Well maintained roads with low values of the displacement Power Spectral Density (PSD) associated with these spatial frequency ranges could reduce significantly the vibration on the sidewalks and, specially, in the vehicle cabin. Finally, a consistent road categorisation for vibration assessment based on the PSD of the pavement irregularity evaluated at the dominant frequencies is proposed.

Keywords: bridge dynamics, pavement irregularity, vibrations, vehicle-bridge interaction models, pedestrians.

INTRODUCTION

The serviceability assessment of traffic-induced vibrations should be performed to guarantee certain comfort levels in road bridges, particularly those which are prone to vibrations induced by heavy vehicles (Camara and Ruiz-Teran 2015; Camara et al. 2014). The analysis of these vibrations is essential for bridges with footpaths because pedestrians have more restrictive comfort levels than drivers and passengers.

The importance of the road pavement profiles on the traffic-induced vibrations has been well documented in recent years. The vertical accelerations measured in the deck and inside the vehicle increase with the amplitude of the pavement irregularities (Marchesiello et al. 1999; Deng and Cai 2009; Deng and Cai 2010; Camara et al. 2014; Camara and Ruiz-Teran 2015), and these are directly related to the users' comfort (Shahabadi 1977). Dodds (Dodds 1972) proposed one of the first categorisations of the road irregularities based on the displacement Power Spectral Density (PSD) of a large number of measured pavement profiles reported by the Motor Industry Research

Association (MIRA) (Labarre et al. 1969):

$$G_d(n) = G_d(n_0)\left(\frac{n}{n_0}\right)^w \tag{1}$$

where $G_d(n)$ is the displacement PSD, $n_0 = 1/2\pi = 0.16$ cycles/m (total wavelength $\lambda_0 = 1/n_0 \approx 6.3$ m/cycle) is the discontinuity frequency (which was defined as independent of the road category) and w (always < 0) controls the slope of the PSD in a logarithmic representation: $w = w_1$ if $n \leq n_0$ and $w = w_2$ if $n > n_0$. Dodds (Dodds 1972) proposed values of the displacement PSD at n_0 ($G_d(n_0)$) and the slopes of the PSD at both sides (w_1 and w_2) for different types of roads, as shown in Fig. 1(a). This definition of the PSD can describe the influence of the road deterioration by reducing the slope of the PSD in the high-frequency range beyond n_0 (i.e. by decreasing the absolute magnitude $|w_2|$) (Dodds and Robson 1973).

More recently, the ISO standard (ISO 8608 1995) simplified the definition of the displacement PSD given in Eq. (1) by proposing a single slope $w = -2$ in the entire frequency domain (i.e. the velocity PSD, G_v, is constant). The value of the displacement PSD (hereafter simply PSD) of the pavement at the reference frequency $n_0 = 0.1$ cycles/m defines the category of the road in terms of its surface irregularities as: $G_d(n_0) = 16 \times 10^{-6}$ for road A (very good quality), $G_d(n_0) = 64 \times 10^{-6}$ for road B (good quality), and $G_d(n_0) = 256 \times 10^{-6}$ for road C (regular quality), all in m^3/cycle. These values correspond to the average of the ranges given by ISO8608 and the resulting PSD is illustrated in Fig. 1(b). However, they are not clearly related to the pavement types used nowadays (i.e. those used in highways, major roads, minor roads, etc.) and the corresponding maintenance standards defined by the infrastructure authorities. In the present work, the PSD of real road profiles with different levels of service life and maintenance is discussed and compared with ISO8608 profiles.

The contribution of different spatial frequency ranges in the road irregularity profiles has a significant impact on the bridge and vehicle vibrations, as well as on the noise induced by the tyre-pavement contact. Different documents report that the spatial frequency band of the pavement between 0.02 cycles/m and 1.4 - 2 cycles/m has the largest contribution to the vertical motion of

vehicles with driving speeds of 70 km/h and 120 km/h (ISO 8608 1995; McLean and Ramsay 1996; Janoff and Mayhoe 1990). Marcondes and his co-authors (Marcondes et al. 1988; Marcondes et al. 1990) observed that the upper limit of vibration frequencies that can cause damage to truck cargo is $f = 50$ Hz. This limit corresponds to a spatial frequency $n = 2$ cycles/m and a vehicle velocity of $V = 90$ km/h (considering that $f = nV$). These results suggest that the band of important pavement frequencies for the vehicle vibration corresponds to what the Permanent International Association of Road Congresses (PIARC) (Descornet 1990) defines as 'roughness' ($n = 0.02 - 2$ cycles/m). Higher-order spatial frequency bands in the pavement surface such as the mega and macrotexture ranges (1000 cycles/m 5 cycles/m) are important for controlling the tyre-pavement noise, as well as the rolling and skid resistance (Descornet 1990). As a result, the spatial frequencies of the road related to noise problems are in principle disconnected to those affecting the vibrations. However, the range of pavement frequencies affected by the new bituminous mixtures employed in maintenance works (aimed to improve the noise comfort) goes beyond the noise emission range and affects the vibration range. Therefore, noise control measures may end up having an impact on the bridge and the vibrational comfort of its users. Addressing this issue is one of the goals of the paper.

From the point of view of the numerical analysis, vehicle-bridge interaction (VBI) models represent the most rigorous approach to assess the level of vibrations and their influence on the comfort of the pedestrians and the vehicle users crossing the bridge (Zhou and Chen 2016). Nevertheless, a representative definition of the pavement surface is essential in order to capture realistically the vibrational phenomenon (Camara and Ruiz-Teran 2015). In VBI models, different vertical displacement records ($r_i(x)$) are imposed to the vehicle wheels to describe the pavement irregularities (Marchesiello et al. 1999; Han et al. 2014). In order to obtain results with statistical meaning, the average from several analyses is obtained using a set of different profiles that are generated by means of a zero-mean stationary Gaussian random process through an inverse Fourier transformation based on the target PSD function (Dodds and Robson 1973):

$$r_i(x) = \sum_{k=1}^{N} \sqrt{2G_d(n_k)\Delta n}\cos\left(2\pi n_k x + \theta_k\right) \tag{2}$$

in which x is the position of the point where the amplitude of the ith-profile of the set (r_i) is defined. The spatial frequencies of the road n_k are considered within the range established by the lower and upper cut-off limits n_1 and n_N, respectively. According to ISO8608, the spatial frequencies below $n_1 = 0.01$ cycles/m (wavelength $\lambda = 100$ m) are not interesting for the study of on-road vehicle vibrations. Most of the research works on VBI follow this recommendation (Camara et al. 2014; Coussy et al. 1989). However, for the study of bridge vibrations (Henchi et al. 1998) proposed a value of n_1 that is related to the span of the bridge (L) so that $n_1 = 1/(2L)$. Regarding the maximum frequency of interest, ISO8608 suggests a value of $n_N = 10$ cycles/m ($\lambda = 0.1$ m/cycle) to indirectly account for the enveloping effect of the tyre, acting as a filter for the road vibration input to the vehicle. This recommendation was followed by many researchers (Marchesiello et al. 1999; Bogsjö et al. 2010; Coussy et al. 1989; Kamash and Robson 1978; Uyls et al. 2007). In a more detailed analysis, (Captain et al. 1979; Chang et al. 2011; Camara et al. 2014) employed a disk model with a rigid tread band that considers explicitly the wheel dimensions and its filtering effects. The selection of the cut-off limits should be related to the structure and the vehicle considered. According to (Coussy et al. 1989) the interval between cut-off frequencies, multiplied by the maximal and minimal speeds chosen for the vehicle, determine a time frequency interval that must contain the most relevant frequencies governing the response (i.e, the important frequencies of the bridge and the vehicle). Δn is the frequency resolution ($\Delta n = 1/L_{\text{prof}}$, where L_{prof} is the length of the profile) and θ_k is a random phase angle uniformly distributed from 0 to 2π to generate a set of independent profiles.

Most of the previous works on VBI adopt a simplistic definition of the road PSD, which can differ significantly from real pavements. This paper investigates the vibrations perceived by users (pedestrians and vehicle users) in a composite bridge under heavy vehicle traffic, focussing the study on the relevance of the pavement description. After presenting the proposed bridge, the vehicle and their interaction, a methodology to obtain suitable displacement profiles based on

measured pavement profiles is detailed. A large number of nonlinear dynamic analyses have been conducted to address the influence of different pavement frequency bands in the vibrations perceived by pedestrians and vehicle users. This is followed by the study of the bridge and vehicle response with different types of pavements, obtained from real road profiles. The results show the large importance of the pavement with spatial frequencies between 0.2 - 1 cycles/m and 0.02 - 0.2 cycles/m for the bridge and the vehicle vibrations, respectively. Finally, a new PSD-based categorisation of road irregularities that is consistent with the observed traffic-induced vibrations is proposed.

DESCRIPTION OF THE BRIDGE AND THE VEHICLE MODELLED

The bridge

This study considers a conventional ladder-deck composite (steel-concrete) bridge with 40 m span and 2 road lanes, as shown in Fig. 2. The total mass of the deck is 738.2 tones (i.e. 7241.7 kN weight), including self-weight, surfacing and parapets. The longitudinal steel beams are supported by POT bearings. The dimensions of the bridge cross-section are illustrated in Fig. 3, where the two sidewalks of the deck are also represented. Hereafter, the sidewalk over transversely fixed supports is referred to as Sidewalk 1, whereas Sidewalk 2 is the one supported by free bearings. The distance between the center of the supports and the girder end is 0.4 m. The joints allow for completely free movements of the girder ends with respect to the abutments. In the Finite Element (FE) model of the bridge, the upper slab is represented by shell elements (approximately 1 m size) that are rigidly connected to the longitudinal and transverse beams that represent the steelwork, accounting for the appropriate offset of the corresponding section centroids. The structural damping is defined by means of a Rayleigh distribution with a 0.5% ratio at the vibration frequencies of 2 and 35Hz in order to ensure that the damping is kept in the range [0.3,0.8]% for the relevant frequencies for the deck vibration in the studied bridge: [18,50] Hz (see next section).

Two 300 m long platforms are connected to the bridge model by means of the joints (0.3 m long). The platforms are required to stabilise the vertical vibration of the vehicle before entering and leaving the bridge. In the numerical model, the platforms are completely rigid up to a distance

of 15 m from the bridge's joints, beyond which the platforms are supported by vertical springs that represent the flexibility of the infill soil, the pavement and the abutment. Fig. 2 shows the position of the platforms and their vertical springs with respect to the bridge. This allows a realistic representation of the hammering effect of the vehicle when entering and leaving the deck, which triggers the bouncing of the vehicle on its suspension.

The vehicle and its interaction with the bridge

The vehicle considered in this study is a 18.6 tonnes HA40 truck proposed by the American Association of State Highway and Transportation Officials' specifications (AASHTO 1998) that is widely employed in VBI studies (Marchesiello et al. 1999; Zhu and Law 2002). The vehicle is modelled with a 7 Degrees-Of-Freedom (DOFs) system that simulates the vertical movement by capturing the pitch, roll and heave rigid body motions of the vehicle body, as well as the flexibility and damping of the tyres and suspensions. The 7 DOFs of the vehicle model are: the vertical displacements of the body, front and rear axles (z_c, z_f and z_r, respectively), the body pitching and rolling motion (θ_c and ϕ_c, respectively) and the front and rear axle rolling (ϕ_f and ϕ_r, respectively). These DOFs are shown in Fig. 3, in which z_u is the vertical displacement of the driver cabin and it is described in terms of the vertical displacement of the vehicle body (z_c) and its pitch (θ_c). The mechanical properties related to the rear and front axles are, respectively: tyre stiffness 1570 and 785 kN/m, tyre damping 0.2 and 0.1 kNs/m, suspension stiffness 373 and 116 kN/m, suspension damping 35 and 25 kNs/m, mass 600 and 1000 kg, and rolling rotary inertia 600 and 550 kgm^2. Referred to the vehicle body, the mass is 17000 kg and the rotary inertias are 13000 and 90000 kgm^2 for the rolling and pitching motions, respectively. The frequencies of the first vibrational modes of the vehicle (f_v) are as follows: (Mode 1) body roll $f_{1,v} = 0.83$Hz, (Mode 2) body pitch $f_{2,v} = 0.92$Hz, (Mode 3) body pitch and heave $f_{3,v} = 1.14$Hz. These modes are represented in Fig. 4(a).

The interaction model between the vehicle and the bridge is defined by means of a friction-less moving contact between the wheels and the shell elements representing the deck and the platforms, where the pavement irregularity is introduced. The interaction problem is established with a non-

linear coupled system of differential equations of motion that is directly integrated step-by-step in the time-domain. This is different from the majority of the previous works on VBI in which the problem is linearised by decomposing the structural response as the superposition of the contribution of different vibrational modes. In this study, the equations of motion are directly integrated in time-domain by means of the HHT implicit algorithm (Hilber et al. 1977) implemented in Abaqus (Abaqus 2011), which allows to capture: (1) second order and nonlinear effects related to the inertial forces developed in the moving vehicle (considered as a multibody dynamic system coupled with the structural motion), (2) the hammering effects of the vehicle at the joints and (3) the eventual loss of the tyre-pavement contact (not observed in this study). A step-time of 0.001s is considered in the analysis. This allows to obtain records of the vertical VBI response that are sufficiently detailed for vibration frequencies below 50 Hz, and also to consider the contribution of high-order spatial frequencies of the irregularities in the tyre-pavement contact.

It was observed in a precursor work that the vibrations on the sidewalks generally increase with the number of vehicles crossing the bridge at the same time (Camara and Ruiz-Teran 2015). Nevertheless, the purpose of this work is to study the influence of the road surface on the vibrations of the bridge and the vehicle, and not to assess the SLS of vibrations of any specific structure. In order to limit the number of computationally expensive analysis, in each of them a single vehicle crosses the bridge centered on Lane 1 at a constant speed of $V = 90$ km/h, having 1.75 m eccentricity with respect to the bridge centreline (see Fig. 2 and 3), which is a realistic load case in the proposed short-span bridge (40 m).

RESPONSE WITH A PERFECTLY FLAT PAVEMENT

First, the VBI is conducted without pavement irregularities (flat road) in order to have a reference value of the accelerations in the deck and the vehicle for the following analyses. Fig. 4(a) presents the Discrete Fourier Transform (DFT) of the vertical accelerations recorded on Sidewalk 1 at midspan (point A in the figure) and at the vehicle cabin (driver side) when crossing the bridge. Part of the free-vibration response, that occurs after the vehicle leaves the deck, is included to complete a 10 s full time-history record. This record length is required in order to provide the

DFT with enough precision for the low-frequency vibrations. The first vibrational mode of the bridge has a frequency of 2.0 Hz and involves the vertical flexure of the deck from abutment to abutment. The moderate participation of this first bridge mode in the accelerations of the deck is clear from Fig. 4(a). However, the first vibrational mode of the bridge influences the response of the vehicle and contributes to the peak in the DFT of its vertical acceleration for frequencies around 2 Hz, well above the first vibrational frequencies of the vehicle (around 1 Hz). The modes that are more relevant for the traffic-induced bridge vibrations in the deck, and therefore for the pedestrian's comfort, are those involving the transverse flexure of the slab in the range between 18 and 50 Hz. This is due to the low transverse flexural stiffness of the deck as a consequence of the large transverse distance between the longitudinal girders (10 m). The vibration of the deck does not interact significantly with that of the vehicle because of the important difference between the dominant frequencies in both responses and the efficiency of the vehicle suspensions in the dissipation of the high-order frequency vibrations of the concrete slab. Fig. 4(b) presents the maximum Root Mean Square (RMS) acceleration on the deck, which is more appropriate than peak acceleration to assess the users' comfort (Boggs and Petersen 1995):

$$a_{\text{RMS}}(t) = \sqrt{\frac{1}{\Delta t_{\text{RMS}}} \int_{t-\Delta t_{\text{RMS}}}^{t} [a(\tau)]^2 \mathrm{d}\tau} \tag{3a}$$

$$\text{RMS} = \max[a_{\text{RMS}}(t)] \tag{3b}$$

where $a(\tau)$ is the vertical acceleration at the time τ and $\Delta t_{\text{RMS}} = 1\text{s}$ is the width of the averaging time interval from which the RMS acceleration ($a_{\text{RMS}}(t)$) at any instant t is obtained. The maximum RMS acceleration, simply referred to as RMS, is obtained as the maximum $a_{\text{RMS}}(t)$ in the complete length of the acceleration record.

Fig. 4(b) shows that the maximum acceleration along the bridge centreline is around 2.5 times larger than on the sidewalks, which verifies the importance of the vibration of the slab between the longitudinal girders. Nevertheless, from the point of view of the pedestrian's comfort, only the

vibration on the footpaths is relevant. The RMS on Sidewalk 1 is approximately 50% lower than that on Sidewalk 2, despite the fact that the former is closer to the vehicle path. This is because the supports in the girder underneath Sidewalk 2 are free to move transversely and it maximises the contribution of the slab modes to the vertical vibration. More details about the effect of the bridge supports on the vehicle-bridge vibrations can be found in (Camara and Ruiz-Teran 2015).

Hereafter, only the RMS at the sidewalk edges is presented, along with the averaged value ($\text{RMS}_{d,c}$) in the entire sidewalks:

$$\text{RMS}_{d,c} = \frac{\sum_j A_j \text{RMS}_j}{\sum_j A_j} \tag{4}$$

where A_j is the area corresponding to the jth-node of the finite element model of the deck and RMS_j its vertical acceleration. The sum is extended along all the nodes at both sidewalks separately to distinguish their response. Table 1 includes the peak, maximum RMS and the averaged $\text{RMS}_{d,c}$ accelerations for the perfectly flat road.

PAVEMENT PROFILES

Several pavement profile measurements were carried out on different roads in service in Spain using a Laser Dynamic PG-LA^{2}IC. It is composed of a commercial high speed profiling laser device designed for quality control and supervision of the road surface, which allowed measuring profiles of the surface course. The equipment was arranged with a sensor type Optocator 2207 and a Laser type LMI/Selcom of 62.5 kHz of frequency. More information about the equipment may be found in (Paje et al. 2013; Vázquez et al. 2016). An encoder was assembled with a magnet on the left rear wheel of a car, giving precision on the distance measured. The surface profile height of the roads was registered at a speed of around 50 km/h. The spacing of the measured data points is $\Delta r = 5$ cm, which is similar to the specifications of the Michigan Department of Transportation and other agencies that specify a data-spacing of approximately 7 cm.

A total of four profiles of flexible pavement irregularities have been measured on-site. In one of the profiles, two different types of pavement where identified: Road 1 with a conventional

pavement type BBTM 11A (650 m long), and Road 2 with the same pavement type and a high content of Crum Rubber (CR) added by the wet process (400 m long). The other three profiles correspond to roads with different levels of deterioration and maintenance. The profiles are labelled according to their visual appearance as: (1) new urban road (298 m long), (2) road with no visual deterioration (386 m long), and (3) road visually deteriorated (386 m long). The new urban road has CR added by the dry process, the other two roads do not include CR additions.

Analysis of the PSD of the measured road profiles

The PSD in real road profiles has a large frequency-to-frequency variability, as shown in Fig. 5(a). The RMS of the profiles' PSD ($G_{d,\text{RMS}}$) is smoothed according to Eq. (5) in order to facilitate the comparison of their frequency content:

$$G_{d,\text{RMS}}(n) = \sqrt{\frac{1}{n_W}\int_{n-n_W/2}^{n+n_W/2} [G_d(\nu)]^2 \, \mathrm{d}\nu} \tag{5}$$

where $G_{d,\text{RMS}}(n)$ is the RMS of the PSD at the spatial frequency n, $G_d(\nu)$ is the PSD of the road profile at the spatial frequency ν within the RMS averaging interval, and $n_W = 0.01$ cycles/m is the averaging width.

Fig. 5(b) compares the smoothed PSD ($G_{d,\text{RMS}}$) of the five measured profiles and the most conventional road categories included in (ISO 8608 1995). Due to the longitudinal spacing between recorded profile points (5 cm), the PSD is limited to spatial frequencies below 10 cycles/m (the Nyquist frequency). As it was echoed by (Marcondes et al. 1990), the PSD proposed by the normative with a constant exponent ($w = -2$) in Eq. (1) cannot describe the entire frequency content of real roads. This is especially evident in the low spatial frequency range of roads with high CR content (Road 2) or new urban profiles with a bituminous CR mixture. In these two cases, there is a clear slope discontinuity (i.e. change in the exponent w) around $n = 1$ cycle/m. In fact ISO8608 recommends the definition of the road category according to the different frequency ranges. However, most of the research works based on VBI analyses generate the road profiles from Eq. (1) without distinguishing different frequency bands. This seems questionable as the

PSD evaluated at the reference frequency $n_0 = 0.1$ cycles/m is not clearly influenced by the maintenance conditions of the road. The new pavement profiles with a high-quality finishing would not be categorised as road A (i.e. the one with better quality) if only $G_d(0.1)$ is considered. An alternative description of the road pavement is suggested in the last part of this study.

Fig. 5(b) proposes a zonification of the frequency range to distinguish between low, intermediate and high-order spatial frequencies (zones 1, 2 and 3 respectively) in light of the relevant changes in the slope of the PSD in the measured profiles. Each zone has been sub-divided into three sub-zones to discuss the influence of the road spatial frequencies in the next sections. It is also remarkable that roads with large levels of deterioration present larger values of the PSD in the range of spatial frequencies between 0.2 and 2 cycles/m, which falls in the PIARC's surface category of 'Roughness' and it is within the range of road frequencies with maximum importance for the vibration (ISO 8608 1995; McLean and Ramsay 1996; Janoff and Mayhoe 1990). The new road and the one with high content of CR (Road 2) maintain relatively large values of the PSD for large spatial frequencies, Zone 3, in comparison with the measured profiles with large degradation.

Implementation of the measured pavement profiles in the numerical model

The measured profiles need to be pre-processed before they can be applied to the VBI model because: (1) a set of 10 independent profiles generated from the same PSD is applied to the wheels on each side of the vehicle ($r_{r,f}^{1,2}$ in Fig. 3) in order to have results with statistical significance, (2) the length of the real road profiles is longer than the length of the bridge and the platforms, and (3) the discontinuities introduced by the bridge joints affect the vibrations and need to be considered by concatenating the profiles corresponding to the platforms and the deck. Consequently, the inverse Fourier transformation in Eq. (2) is employed to generate sets of independent profiles for the platforms and the bridge from either the $G_{d,\text{RMS}}$ in real profiles, or from Eq. (1) for idealised ISO8608 profiles. The upper cut-off frequency of $n_N = 10$ cycles/m for the measured profiles is extended to $n_N = 30$ cycles/m in the generation of the synthetic ISO profiles in order to account for the influence of the high-order road frequencies (zone 4). The profiles that are included in the VBI model are generated from Eq. (2) to match the PSD of the measured (or the ISO8608) pavement

irregularities with $\Delta r = 1$ cm spacing. This value is lower than that in the measured profiles (5 cm) in order to provide enough accuracy in zone 3 (below $n = 10$ cycles/m) and allow for the estimation of the influence of zone 4 in the ISO profiles ($\Delta r = 1$ cm gives 3 points of the profile for each cycle of the upper cut-off frequency $n_N = 30$ cycles/m). The lower cut-off frequencies are expected to be different in the bridge and in the approaching platforms due to the different construction stages and the deflection of the bridge under permanent loads. The lower cut-off frequencies in the platforms and in the bridge are $n_1 = 0.01$ and $n_1 = 1/2L = 0.0125$ cycles/m (where $L = 40$ m), respectively (Henchi et al. 1998). The frequency resolution is $\Delta n = n_1$. Once the profiles are generated they are concatenated at the joints as represented in Fig. 6. It is assumed that there is no construction misalignment and that the joint is perfectly flat. Two of the profiles generated from the $G_{d,\text{RMS}}$ of the new urban profile and the highly deteriorated road are illustrated in Fig. 6(a), where it is observed that the irregularity amplitudes in the highly deteriorated roads can be up to two times those in the new urban profiles.

The effect of the wheel dimensions in the pavement profiles is explicitly considered in this work by filtering the generated profiles using the rigid disk model shown in Fig. 6(b) (Chang et al. 2011; Camara et al. 2014). This model is deemed to be more accurate than the arbitrary reduction of the upper cut-off frequency to $n_N = 10$ cycles/m that is routinely adopted to simplify the wheel effects. Note that the proposed filtering model considers the wheels as rigid disks, but the VBI model includes their flexibility and damping through the springs and dashpots represented in Fig. 3. Furthermore, previous works concluded that the vehicle response is similar using the rigid disk or more refined models in which the tyre-pavement contact is defined as a rectangular patch with finite dimensions (Captain et al. 1979). Nevertheless, the filtering effect is small as it is shown in the profiles at the bridge joints in Fig. 6(b). This is because the contact point between the wheel and the pavement (point P in this figure) is almost aligned vertically with the wheel's centre (point O) due to the small amplitude of the irregularities with respect to the wheel radius: 30 cm. After examining the PSD resulting from the filtered profiles, it is concluded that the effect of the wheel dimensions is only noticeable for frequencies above 7 cycles/m in the case of deteriorated roads.

INFLUENCE OF THE PAVEMENT FREQUENCY CONTENT ON THE ACCELERATIONS

The goal of this part of the study is to find the road frequencies, or frequency ranges, that are more relevant in the traffic-induced vibration perceived from the bridge users'. First, different sets of 10 independent profiles have been generated from the code-based PSD in Eq. (1) by including only one spatial frequency in Eq. (2) (i.e. $N = 1$). The ISO8608 road category B ($G_d(n_0 = 0.1) = 64 \times 10^{-6}$ m^3/cycle) is considered in this section because its PSD at n_0 is close to most of the profiles measured on-site (see Fig. 5(b)). The same profiles are applied to the two lateral wheel lines of the vehicle in order to maximise its vertical response (i.e. $r^1 = r^2$ in Fig. 3).

Fig. 7(a) presents the ratio between the RMS acceleration obtained with the single-frequency pavement profiles (arithmetic mean of the 10 records) and that obtained from the perfect road, both in the bridge and the vehicle. It is clear that the vehicle is more sensitive to changes in the frequency content of the road surface, particularly at the frequencies associated with its roughness, but not with its texture (according to the PIARC's classification). Only the frequencies of the pavement between 0.014 and 0.50 cycles/m (zones from 1A to 2B) influence significantly the vehicle response. Fig. 7(a) shows that up to 98% of the mean acceleration that is registered in the cabin when the pavement includes the whole frequency range (Road B) can be achieved by activating exclusively the pavement frequencies that coincide with the first two pitching modes of the vehicle. The vibration frequency f can be translated to spatial frequency using: $n_{i,v} = f_{i,v}/V$, where $V = 90$ km/h is the vehicle velocity and $i = 2, 3$ refer to the first and the second vehicle pitching modes. The response of the vehicle is rapidly attenuated by increasing the pavement frequency beyond the vehicle pitching modes, but there is a frequency band around 0.1 cycles/m in which the pavement contributes significantly to the interaction between the vehicle and the bridge. This frequency band is highlighted in grey colour in Fig. 7(a) and it is clearly connected to the frequency content of the vehicle's response presented in Fig. 4(a). It is also interesting to look at the effect of the longitudinal distance between wheel axles in the vehicle ($L_v = 4.73$ m, Fig. 3). Regardless of the vehicle velocity, its pitch movement will be activated if the road irregularity

induces a vertical movement in the front wheels that is completely out-of-phase with respect to the rear ones: $n_{v,\text{pitch}} = 1/(L_v/2) = 0.105$ cycles/m. On the other hand, a pure in-phase movement of the front and the rear axles will excite the heave motion of the vehicle: $n_{v,\text{heave}} = 1/L_v = 0.210$ cycles/m. By comparing the response of the vehicle when the pavement has only one of these two frequencies, its is clear that the heave motion has less importance than the pitch in terms of the acceleration in the cabin, which is attributed to the significant distance between the gravity center and the cabin in the AASHTO vehicle (3.153 m). Fig. 7(a) also includes the pavement spatial frequency related to the vibrational mode of the bridge with the largest contribution to its RMS accelerations ($n_{d,b} = 18.1/V = 0.72$ cycles/m). This pavement frequency has a negligible impact on the vehicle response, and also on the bridge acceleration, when it is the only frequency activated in the pavement profile. Considering the combination of these effects, the most important range of pavement spatial frequencies for the vehicle vibration falls between 0.02 and 0.2 cycles/m (zones 1B - 2A).

Fig. 7(a) suggests that including a single spatial frequency in the pavement profile is not adequate to study the influence of the pavement on the deck vibration. The response of the bridge is controlled by a wide range of vibrational modes and, therefore, the pavement profile should be generated with multiple spatial frequencies in order to explore the vibration on the sidewalks. To this end, instead of activating certain road frequencies, the pavement is now generated by cancelling each of the 10 frequency bands proposed in Fig. 5(b) (1A, 1B, ... 3B, 3C, and 4) and including all the others. These sub-zones have been distributed with approximately constant width in the logarithmic plot. Consequently, employing a linear distribution of frequencies in Eq. (2) would lead to an unbalanced number of PSD target points between sub-zones. This has been avoided by defining a logarithmic distribution of frequencies in Eq. (2), imposing that the profiles are generated with the same number of frequencies (300) in all the sub-zones. It has been observed that the vibrations in the deck and the vehicle with road profiles generated from this logarithmic distribution of frequencies is statistically the same as that obtained with the linear distribution, validating this approach.

Fig. 7(b) presents the ratio between the average $\text{RMS}_{d,c}$ acceleration induced by the standard Road B profiles and that considering road B profiles with different frequency ranges cancelled. In this case the reference response is the one obtained with the profiles that include the whole frequency range (Road B) in order to highlight that specific frequency bands increase the vertical vibration of the bridge when this ratio is above 1. Considering a perfectly flat pavement (i.e. all the frequencies are cancelled) the $\text{RMS}_{d,c}$ decreases by 18 and 13% in Sidewalks 1 and 2, respectively. Fig. 7(b) shows that the frequency bands with larger contribution to the vibration of the bridge are between 0.2 and 1 cycles/m (zones 2B and 2C). By cancelling one of these frequency bands in the generation of the road profiles, the $\text{RMS}_{d,c}$ average acceleration is around 6% smaller than the result obtained with all the frequencies (Road B). The result can be explained by the important contribution to the response on the sidewalks of the first slab modes of the bridge, around 18 Hz (see Fig. 4(a)), which means that the equivalent spatial frequency of this vibrational bridge mode is 0.7 cycles/m for a vehicle velocity of 90 km/h, corresponding to Zone 2C. Considering a range of reasonable vehicle velocities in highways (60 - 120 km/h) the resulting dominant frequency would be in the range between 0.5 and 1 cycles/m (zone 2C), which is in agreement with the values presented in Fig. 7(b). This result should be referred to the dominant modes of the studied bridge and it is within the band of important frequencies suggested by previous research works and normative (between 0.02 cycles/m and 2 cycles/m) (ISO 8608 1995; McLean and Ramsay 1996; Janoff and Mayhoe 1990).

INFLUENCE OF THE ROAD QUALITY AND REPARATION

This section focuses on the response of the bridge and the vehicle considering real pavements that are generated independently for the right and left wheels (i.e. $r^1 \neq r^2$) from the $G_{d,\text{RMS}}$ of the real roads. Fig. 8 shows the arithmetic mean of the maximum RMS acceleration on Sidewalks 1 and 2 for the different pavement profiles. The coloured bands centered in the mean response represent one standard deviation of the results for the 10 profiles considered in each case. Fig. 8(a) compares the vibration on the bridge sidewalks for roads with different CR content. It is observed that the road with high CR content (Road 2) leads to reduced vibrations along both sidewalks.

The accelerations resulting from Road 2 are almost identical to those observed with the perfect road. Fig. 8(b) shows the acceleration on the sidewalks for irregularity profiles with different deterioration levels. The accelerations with the new urban pavement and the one with no visual deterioration are very similar to those with a perfectly flat road. However, the vehicle crossing the highly deteriorated road induces accelerations on the sidewalks that are appreciably larger than with other roads, the difference being above one standard deviation. The stronger induced vibrations observed with the highly deteriorated road and with Road 1 (unrepaired pavement) can be explained by the significantly larger values of the PSD of these roads in zones 2B and 2C, in comparison with the other roads. These two frequency bands were identified as the most contributing ones for the bridge vibrations in the previous section. Table 1 summarises the peak, maximum RMS and average $\text{RMS}_{d,c}$ acceleration on both sidewalks for different profiles. Roads with high CR content slightly reduce the vibrations perceived by pedestrians, approximately by 10%, in comparison with highly deteriorated roads. This effect is not due to the modification of the flexibility of the pavement by the CR addition, which is negligible and not accounted for in the numerical model, but rather to the modification of its texture, as shown in Fig. 5.

The arithmetic mean of the peak and maximum RMS accelerations in the cabin for different roads are summarised in Table 1, where the large sensitivity of the vehicle response to the road irregularities is observed. In comparison with the new urban profile, the RMS acceleration in the cabin is 20% larger with the visually deteriorated pavement but it increases up to 70% with the road without apparent deterioration. This is further explored in Fig. 9, where the time-history evolution of the acceleration in the vehicle cabin is shown. It is observed that the road with no visual deterioration magnifies the vibration in the vehicle in comparison with other roads, even the one with apparent deterioration. This is explained by the large PSD of the non-deteriorated road in zone 1C, where the frequencies of the dominant vehicle pitching modes are contained (see Fig. 7(a)). Table 1 shows that changing from Road 1 to 2, and therefore reducing the PSD of the road in zones 1 and 2, the vertical acceleration on the deck is only reduced by approximately 5% but the RMS acceleration in the vehicle cabin is reduced down to 44%. This verifies that the contribution

to the vehicle vibration of the low-order frequencies of the pavement roughness, especially in zone 1C, is larger than that of the high-order frequencies associated with the megatexture of the road surface (larger than 2 cycles/m).

Table 1 also includes the acceleration in the vehicle and the bridge for the ISO8608 Road B. The acceleration on the sidewalks of the deck with this idealised road is larger than with any of the real profiles, even those with significant deterioration. This can be explained by the larger PSD of Road B in the range of important frequencies for the deck acceleration (zones 2B and 2C). However, the vibration in the vehicle cabin is larger with the existing Road 1 and with the measured profiles corresponding to the deteriorated and not deteriorated roads. These three pavements present PSD values that are above those anticipated by the code-based Road B in the range of relevant modes for the vehicle vibration (zones 1B and 1C), which may explain this result.

Proposed spatial frequencies for road categorisation in terms of user's comfort

Table 1 presents the PSD ($G_{d,\text{RMS}}$) evaluated at the reference frequency proposed by (ISO 8608 1995), and puts it in relation to the vibrations in the deck and the vehicle for the corresponding road profiles. The road that is visually not deteriorated, which also presents the lowest value of $G_{d,\text{RMS}}(n_0 = 0.1)$ among all the roads, is the one that induces the largest level of vibration in the vehicle. This remarks the reduced influence of the ISO reference frequency of the pavement, $n_0 = 0.1$ cycles/m, on the vibration of the AASHTO truck and it suggests that defining the road category in terms of $G_{d,\text{RMS}}(n_0 = 0.1)$ would not be appropriate for the vibration assessment of this specific vehicle.

Indeed, the most important spatial frequencies of the pavement for the vehicle vibration are the ones related to its dominant vibrational frequencies ($f_{d,v}$) and its velocity (V), i.e. $n_{d,v} = f_{d,v}/V$ as shown in Section 5. Consequently, it is proposed to consider the PSD evaluated at the pavement spatial frequency corresponding to the first pitching mode of the vehicle, $n_{d,v}$ (i.e. $G_{d,\text{RMS}}(n_{d,v})$), as a meaningful parameter to assess the quality of the road from the point of view of the vehicle users' comfort. The dominant spatial frequency $n_{d,v}$ should be selected according to the representative traffic crossing the bridge. In order to assess the validity of this proposal for

different vehicle typologies, the stiffness of the original AASHTO vehicle's suspensions has been modified to achieve a fundamental pitching mode of the vehicle of 5 and 12.5 Hz, which coincides with spatial frequencies of 0.2 and 0.5 cycles/m when the driving speed is 90 km/h, respectively. Fig. 10 presents the peak RMS acceleration in the vehicle's cabin for the measured road profiles in terms of $G_{d,\text{RMS}}(n)$, where n is the spatial frequency of the first pitching mode of the vehicle ($n = n_{d,v}$, i.e. the proposed parameter) or the reference ISO frequency ($n = n_0 = 0.1$ cycles/m). It is observed that increments of $G_{d,\text{RMS}}(n_{d,v})$ in the road PSD are typically associated with higher levels of the vehicle acceleration, representing a more robust indicator of the road quality in terms of vehicle user's comfort than $G_{d,\text{RMS}}(n_0)$, which is not directly connected to the vibrations in the vehicle. This is particularly clear for roads with low values of the PSD at n_0, i.e. those with no visual deterioration but with significant vehicle vibration. Note that the emphasis in Fig. 10 is exclusively on the relationship between the vertical acceleration of the vehicle and the road's PSD at certain frequencies, but not on the magnitude of the accelerations. These are unrealistically high for the modified vehicles included in Fig. 10(b).

Regarding the pedestrian's comfort, it would be convenient to evaluate the RMS PSD of the road at the spatial frequency corresponding with the dominant vibrational mode of the bridge for the accelerations on the sidewalks: $n_{d,b} = f_{d,b}/V$, in which the governing bridge frequency $f_{d,b}$ can be obtained from DFT analyses of the acceleration records, as shown in Fig. 4(a). In this case $f_{d,b} = 18.1$ Hz and $n_{d,b} = 18.1/(90/3.6) = 0.72$ cycles/m, which is included in Fig. 5(b). Table 1 also presents the PSD at this frequency, $G_{d,\text{RMS}}(n_{d,b})$, and the results suggest that the higher this value the larger the vibrations on the sidewalks, which suggests that it is a consistent parameter to categorise the road pavement in terms of the pedestrian's comfort.

CONCLUSIONS

An extensive numerical analysis supported by on-site pavement measurements is conducted in this work to address the vertical vibrations that affect the users of road bridges. The irregularities of the pavement are obtained from real road measurements and also from the Power Spectral Density (PSD) of displacements suggested by (ISO 8608 1995). Different sets of pavement profiles

are generated for a conventional 40 m span composite ladder deck bridge and its approaching platforms. The filtering effect of the vehicle wheels is considered in the profiles, which are connected at the bridge joints to model these discontinuities.

The results indicate that the vertical accelerations induced on the deck by the vehicle riding on the code-defined pavement with 'good quality' (Road B) are clearly above those obtained with any of the real road profiles measured on-site. After comparing the results for several road pavements and vehicles with different dominant frequencies, it is observed that the traffic-induced vibrations on the bridge and in the vehicle cabin are directly related to the RMS of the PSD ($G_{d,\text{RMS}}$) evaluated at the dominant spatial frequencies for the deck ($n_{d,b}$) and for the vehicle ($n_{d,v}$) vibration, respectively. Consequently, it is proposed to categorise the road pavement in terms of the traffic-induced vibrations based on $G_{d,\text{RMS}}(n_{d,b})$ and $G_{d,\text{RMS}}(n_{d,v})$.

The frequency content of the road irregularities has a significant impact on the bridge and vehicle vibrations. Resonant effects that magnify the vertical accelerations are observed for large values of the road PSD at frequencies close to the dominant vibrational modes of the bridge and, especially, the vehicle. Considering a conventional scenario for vibration assessment in which a 18.6 tones truck crosses a 40-m span composite bridge (dominated by slab modes between 18 and 50 Hz) at 90 km/h, the most relevant road frequencies for the bridge vibration are contained in the interval between 0.2 and 1 cycles/m. The PSD measured in existing roads indicates that this frequency range is especially sensitive to the pavement deterioration. Regarding the vehicle response, its vertical cabin acceleration is strongly influenced by the pavement irregularities with frequencies in the range of 0.02 and 0.2 cycles/m, particularly those that match the vehicle pitching modes (for the specific driving velocity). These results emphasises the importance of an strategic pavement maintenance on the deck that targets the PSD at these frequency bands.

Highly deteriorated pavements increased by 12% and 20% the RMS vibrations on the sidewalks and in the vehicle cabin, respectively, when compared with a new road. It is also observed that a high content of Crumb Rubber (CR) in the pavement reduces the acceleration on the sidewalks of the bridge (around 5%), but specially in the vehicle cabin (up to 44%). This is attributed to the

modification of the pavement roughness in a range of spatial frequencies between 0.02 and 0.2 cycles/m that affects the vehicle vibration. However, these frequencies are well below the ones related to tyre-pavement noise reduction (5-1000 cycles/m), which is one of the main purposes of the addition of CR.

Although the results suggest that the traffic-induced vibration and noise are not directly connected, it is essential to understand how to design road pavements and their maintenance programmes in order to maximise the user's comfort and to minimise the noise pollution at the same time. This study suggests further multi-disciplinary research works that employ pavement profiles with 1 or 2 mm data-spacing and smaller step-times, thus allowing for the accurate study of spatial frequencies up to 250 cycles/m.

ACKNOWLEDGEMENTS

The authors would like to express their gratitude to Imperial College London for the Elsei Widdowson Fellowship Award given to the third author, which has partially funded the first author position at this institution when this research work was conducted. The financial support from MINECO (Spain) and FEDER through project TRA2016-77418-R is also greatly appreciated, as well as the support from the IMPACT FUND 2016-2017 award from City, University of London.

REFERENCES

AASHTO (1998). "Load and resistance and factor design: Bridge design specifications." *American Association of State Highway and Transportation Officials*. 2nd Edition.

Abaqus (2011). "Finite element analysis program; version 6.11. Providence USA.

Boggs, D. and Petersen, C. (1995). "Acceleration indexes for human comfort in tall buildings - peak or rms?

Bogsjö, K., Podgorsky, K., and Rychlik, I. (2010). *Models for road surface roughness*. University of Gothemburg, Dept. Mathematical Sciences.

Camara, A., Nguyen, K., Ruiz-Teran, A., and Stafford, P. (2014). "Serviceability limit state of vibrations in under-deck cable-stayed bridges accounting for vehicle-structure interaction." *Engineering Structures*, 61, 61 – 72.

Camara, A. and Ruiz-Teran, A. (2015). "Multi-mode traffic-induced vibrations in composite ladder-deck bridges under heavy moving vehicles." *Journal of Sound and Vibration*, 355, 264 – 283.

Captain, K., Boghani, A., and Wormley, D. (1979). "Analytical tire models for dynamic vehicle simulation." *Vehicle System Dynamics*, 8, 1–32.

Chang, K., Wu, F., and Yang, Y. (2011). "Disk model for wheels moving over highway bridges with rough surfaces." *Journal of Sound and Vibration*, 330, 4930–4944.

Coussy, O., Said, M., and Van Hoove, J. (1989). "The influence of random surface irregularities on the dynamic response of bridges under moving loads." *Journal of Sound and Vibration*, 130(2), 313–320.

Deng, L. and Cai, C. (2009). "Identification of parameters of vehicles moving on bridges." *Engineering Structures*, 31(10), 2474 – 2485.

Deng, L. and Cai, C. (2010). "Development of dynamic impact factor for performance evaluation of existing multi-girder concrete bridges." *Engineering Structures*, 32(1), 21 – 31.

Descornet, G. (1990). *Reference road surfaces for vehicle testing*. Roads PIARC, No. 272.

Dodds, C. (1972). *Generalised terrain dynamic inputs to vehicles*. BSI Document 72/34562

(ISO/TC/108/WG9 (MEE/158/3/1)).

Dodds, C. and Robson, J. (1973). "The description of road surface roughness." *Journal of Sound and Vibration*, 31(2), 175–183.

Han, W., Wu, J., Cai, C., and Chen, S. (2014). "Characteristics and dynamic impact of overloaded extra heavy trucks on typical highway bridges." *Journal of Bridge Engineering*, 20(2), 05014011–1/11.

Henchi, K., Fafard, M., Talbot, M., and Dhatt, G. (1998). "An efficient algorithm for dynamic analysis of bridges under moving vehicles using a coupled modal and physical components approach." *Journal of Sound and Vibration*, 214(4), 663 – 683.

Hilber, H., Hughes, T., and Taylor, R. (1977). "Improved numerical dissipation of time integration algorithms in structural dynamics." *Earthquake engineering and structural dynamics*, 5, 283–292.

ISO 8608 (1995). "Mechanical vibration - Road surface profiles - Reporting of measured data." *International Organization for Standardization (ISO)*.

Janoff, M. and Mayhoe, G. (1990). "The development of a simple instrument for measuring pavement roughness and predicting pavement rideability." *Report no.*, Surface Characteristic of Roadways: International Research and Technologies. ASTM, STP 1031.

Kamash, K. and Robson, J. (1978). "The application of isotropy in road surface modelling." *Journal of Sound and Vibration*, 57(1), 89–100.

Labarre, R., Forbes, R., and Andrew, S. (1969). *The measurement and analysis of road surface roughness*. Motor Industry Research Association, report No. 1970/5.

Marchesiello, S., Fasana, A., Garibaldi, L., and Piombo, B. (1999). "Dynamics of multi-span continuous straight bridges subject to multi-degrees of freedom moving vehicle excitation." *Journal of Sound and Vibration*, 224(3), 541 – 561.

Marcondes, J., Burgess, G., Harichandran, R., and Snyder, M. (1990). "Spectral analysis of highway pavement roughness." *Journal of Transportation Engineering*, 117(5), 540 – 549.

Marcondes, J., Singh, S., and Burgess, G. (1988). "Dynamic analysis of a less than truck load

shipment." *Paper 88-WA/EEP-17, ASME*, New York.

McLean, J. and Ramsay, E. (1996). "Interpretations of road profile-roughness data: review and research needs." *Report no.*, ARRB Transport Research report, ARR 295.

Paje, S., Luong, J., Vázquez, V., Bueno, M., and Miro, R. (2013). "Road pavement rehabilitation using a binder with a high content of crumb rubber: Influence on noise reduction." *Journal of Construction and building Materials*, 47, 789 – 798.

Shahabadi, A. (1977). "Bridge vibration studies. joint highway research project." *Report no.*, Purdue University & Indiana State Highway Commission (September). Rep. No. JHRP 77-17.

Uyls, P., Els, P., and Thoresson, M. (2007). "Suspension settings for optimal ride comfort of off-road vehicles travelling on roads with different roughness and speeds." *Journal of Terramechanics*, 44, 163 – 175.

Vázquez, V., Luong, J., Bueno, M., Terán, F., and Paje, S. (2016). "Assessment of an action against environmental noise: Acoustic durability of a pavement surface with crumb rubber." *Science of The Total Environment*, 542, Part A, 223 – 230.

Zhou, Y. and Chen, S. (2016). "Vehicle ride comfort analysis with whole-body vibration on long-span bridges subjected to crosswind." *Journal of wind engineering and structural dynamics*, 155, 126–140.

Zhu, X. and Law, S. (2002). "Dynamic load on continuous multi-lane bridge deck from moving vehicles." *Journal of Sound and Vibration*, 251(4), 697 – 716.

NOTATION

Main symbols employed in this paper and corresponding SI units:

G_d = Displacement Power Spectral Density (PSD) [m^3/cycle];

$G_{d,\mathrm{RMS}}$ = Root Mean Square (RMS) of the displacement PSD [m^3/cycle];

n = spatial frequency [cycles/m];

n_0 = code-defined reference spatial frequency [cycles/m];

$n_{d,b}$ = dominant spatial frequency for bridge vibrations [cycles/m];

$n_{d,v}$ = dominant spatial frequency for vehicle cabin vibrations [cycles/m];

n_1 = lower cut-off frequency for pavement generation [cycles/m];

n_N = upper cut-off frequency for pavement generation [cycles/m];

n_W = averaging window width in the calculation of $G_{d,\mathrm{RMS}}$ [cycles/m];

Δn = frequency resolution [cycles/m];

w = slope of the displacement PSD in logarithmic coordinates;

L = span of the bridge [m];

V = vehicle velocity [m/s];

f = natural frequency of vibration [Hz];

$r(x)$ = vertical displacement amplitude of the pavement profile at a distance x [m];

Δr = data spacing of the pavement profile [m];

L_{prof} = Pavement profile length [m];

a_{RMS} = Root Mean Square (RMS) vertical acceleration [m/s^2];

Δt_{RMS} = averaging window width in the calculation of a_{RMS} [s];

$\mathrm{RMS}_{d,c}$ = Root Mean Square (RMS) vertical acceleration averaged on the sidewalks [m/s^2].

List of Tables

TABLE 1. Accelerations for different road qualities presented as the arithmetic mean for the sets of 10 profiles, in units of m/s^2. The RMS displacement PSD ($G_{d,\mathbf{RMS}}$) at different frequencies is included in mm^3/cycle.

		Perfect road	Road B ISO8608	Road 2	Road 1	New urban	Visually not deteriorated	Visually deteriorated
SW1[a]	Peak	2.20	2.34	2.22	2.30	2.23	2.23	2.28
	RMS	0.74	0.85	0.75	0.79	0.74	0.75	0.78
	$\text{RMS}_{d,c}$	0.33	0.39	0.35	0.37	0.33	0.34	0.37
SW2[b]	Peak	5.45	5.36	5.36	5.21	5.53	5.63	5.53
	RMS	1.28	1.46	1.30	1.36	1.30	1.33	1.38
	$\text{RMS}_{d,c}$	0.49	0.56	0.50	0.53	0.49	0.50	0.53
Driver	Peak	2.22	3.34	2.96	6.11	2.96	4.96	3.62
	RMS	1.10	1.31	1.31	2.34	1.32	2.25	1.59
$G_{d,\text{RMS}}(n_0)$		0	0.06	0.06	0.70	0.10	0.04	0.10
$G_{d,\text{RMS}}(n_{d,v})$		0	0.40	0.07	0.60	0.09	1.09	0.60
$G_{d,\text{RMS}}(n_{d,b})$		0	$1.2{\cdot}10^{-3}$	$1.0{\cdot}10^{-4}$	$7.0{\cdot}10^{-4}$	$2.5{\cdot}10^{-5}$	$5.0{\cdot}10^{-5}$	$3.2{\cdot}10^{-4}$

[a]Sidewalk 1. [b]Sidewalk 2.

List of Figures

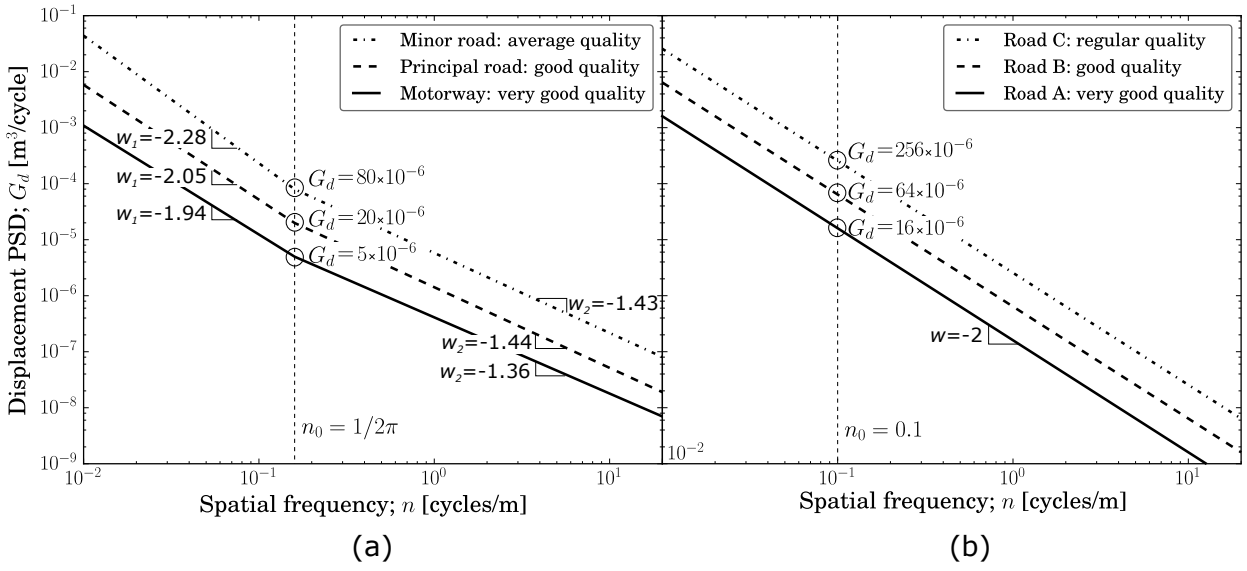

FIG. 1. Definition of the displacement PSD for different road categories (considering the mean values of w and $G_d(n_0)$): (a) Dodds (1972), (b) ISO8608.

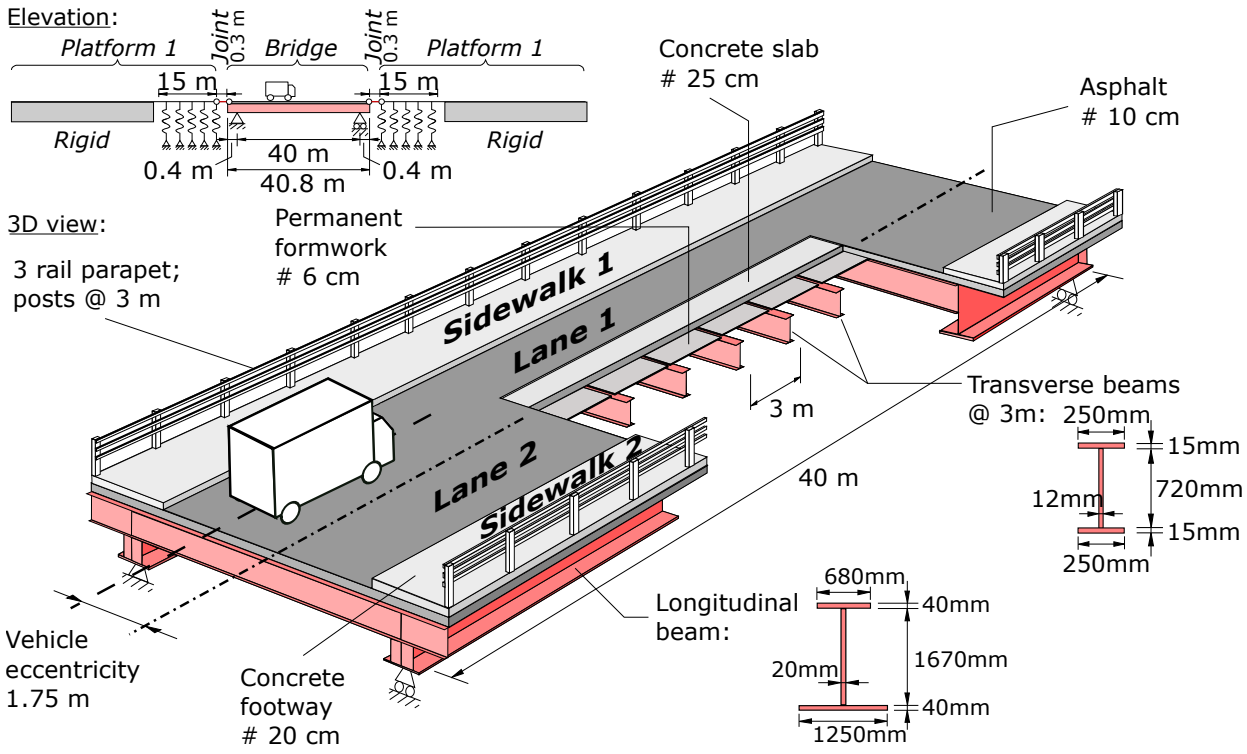

FIG. 2. Schematic three-dimensional (3D) view of the composite bridge. The elevation of the structure and the platforms is also included. Note that in the numerical model the region with 'rigid' platforms has infinite vertical stiffness, regardless of the type of pavement.

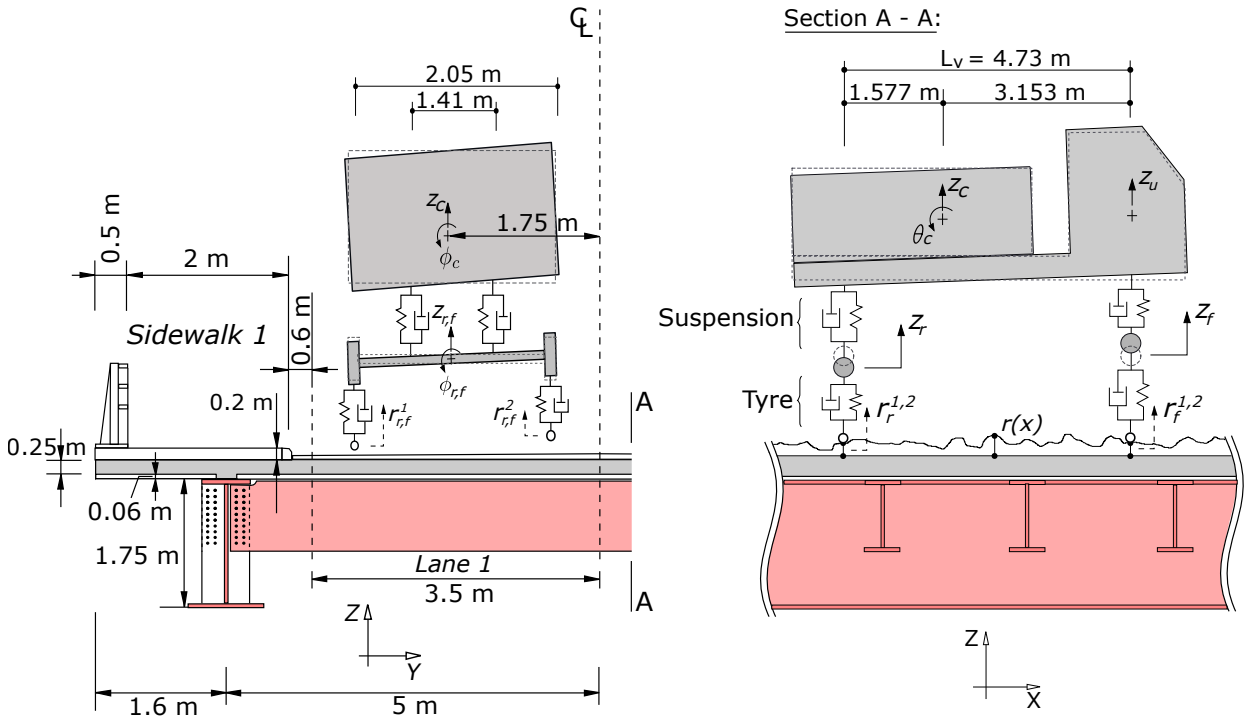

FIG. 3. Cross-section and elevation of the bridge. The 7-DOFs vehicle model and the road irregularity (with exaggerated amplitude for illustration purposes) are included.

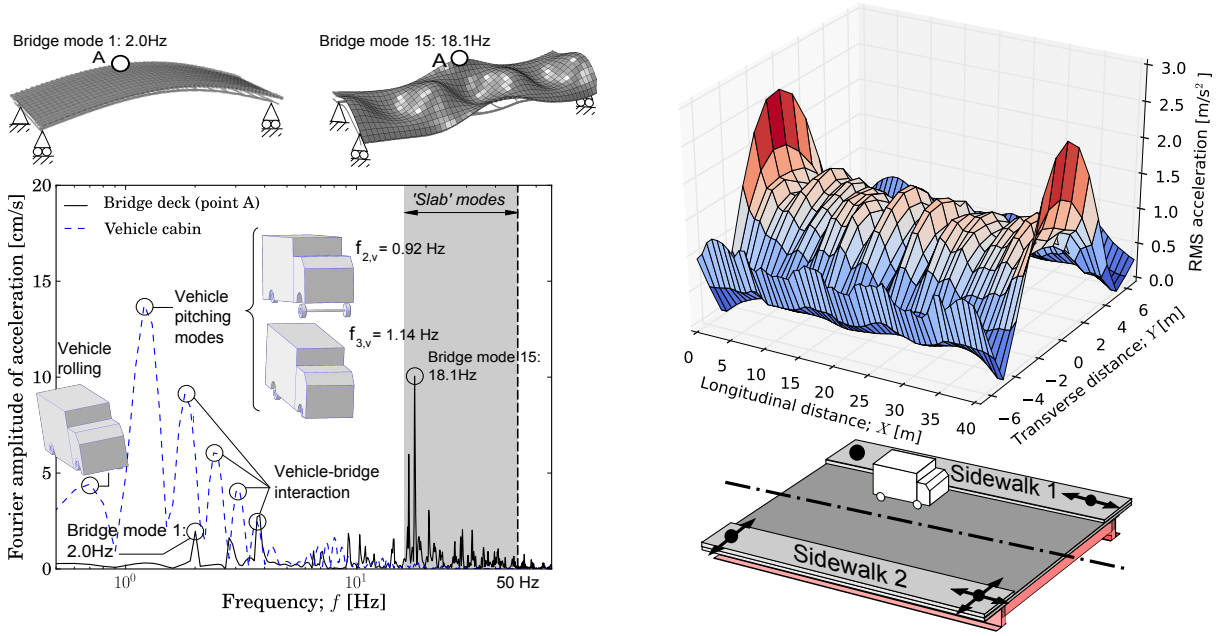

(a) (b)

FIG. 4. Vibrational response for a perfectly flat pavement: (a) frequency content of the vertical acceleration on the bridge (Sidewalk 1 at midspan, point A) and the vehicle cabin, (b) maximum RMS accelerations on the entire deck (the degrees of freedom of the POT supports are included).

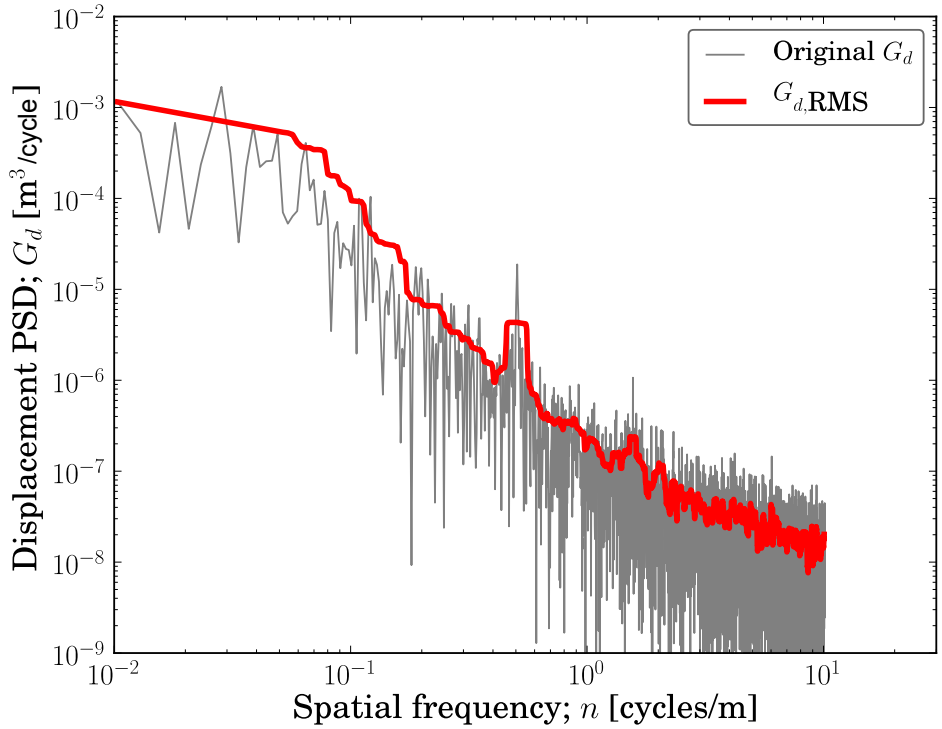

(a)

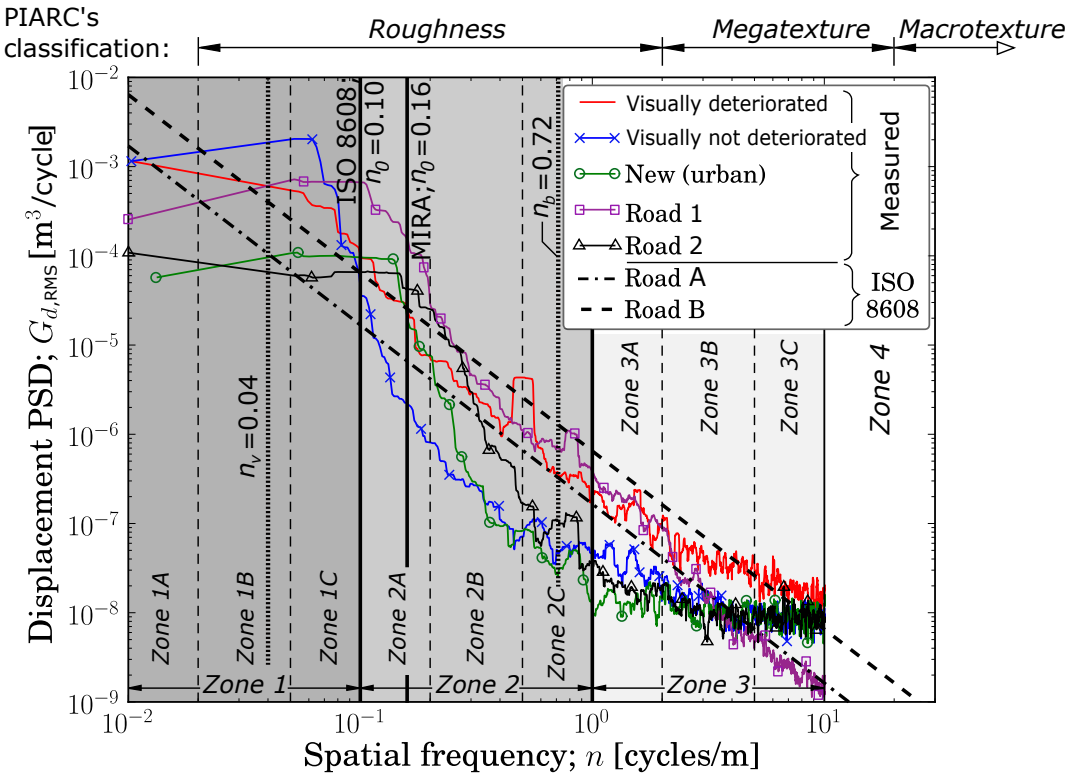

(b)

FIG. 5. PSD (G_d) of the measured road irregularities: (a) RMS of G_d in the deteriorated road, (b) proposed frequency range zonification for vehicle-bridge vibrations.

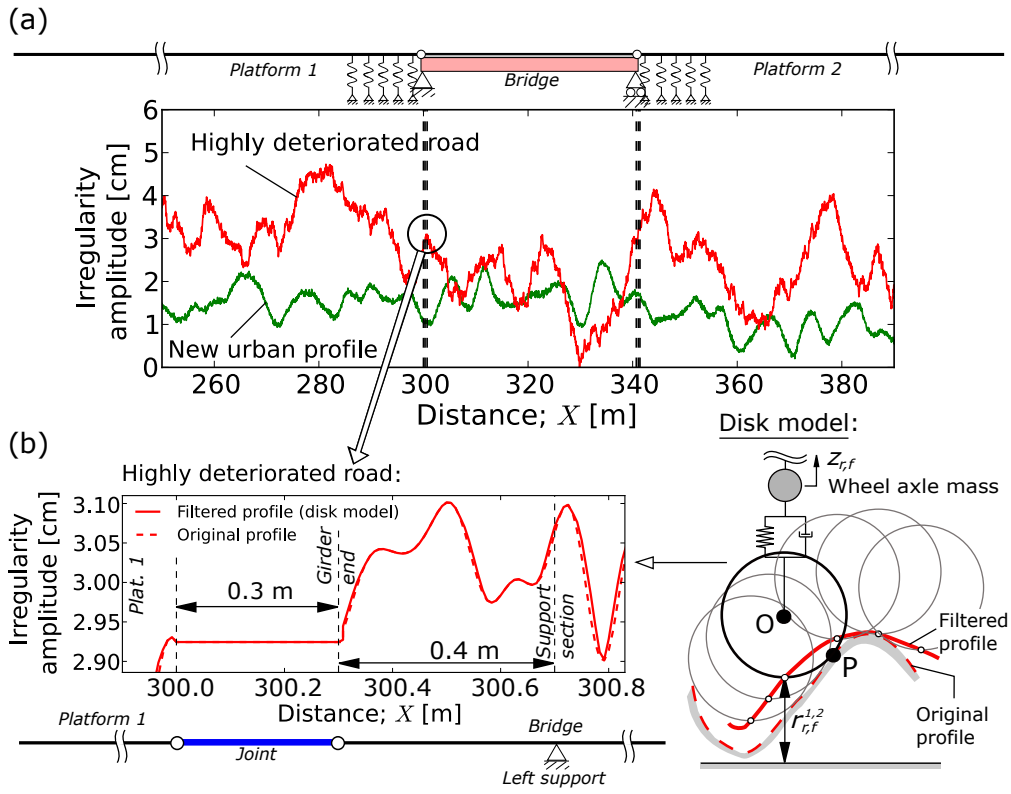

FIG. 6. Road irregularities: (a) Two road profiles generated from the measured $G_{d,\mathrm{RMS}}$. (b) Detail of the concatenation of profiles at the joint and the filtering effect of the wheels (disk model).

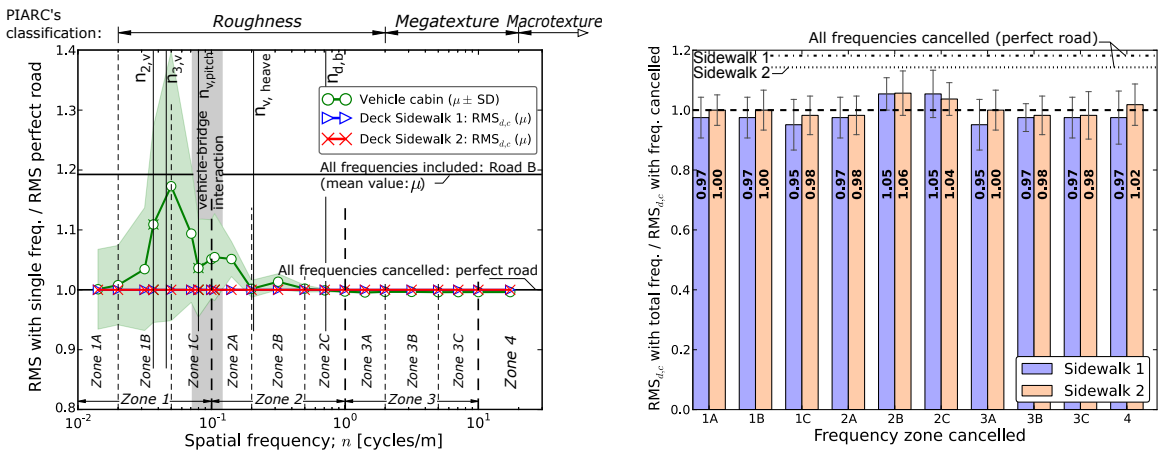

(a) (b)

FIG. 7. Influence of the frequency content of the pavement irregularity by: (a) including a single frequency in the profile generation, and (b) cancelling a frequency band. The results represent the arithmetic mean (μ) and the standard deviation (SD) with a coloured band (Fig. (a)) or with error bars (Fig. (b)).

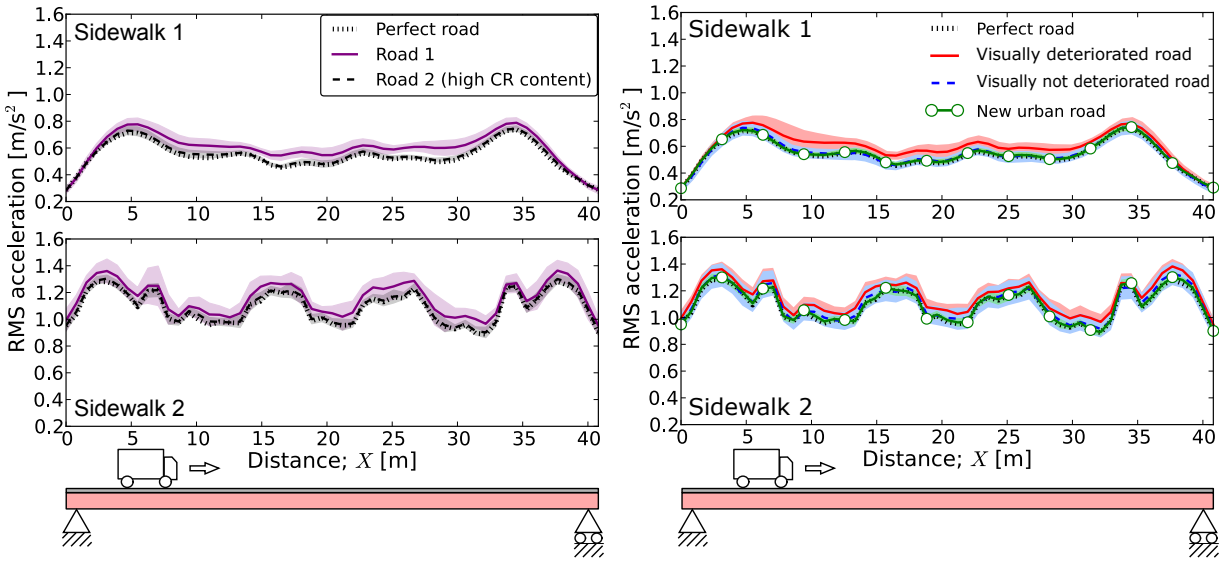

(a) (b)

FIG. 8. Maximum RMS acceleration along the sidewalks (edges) for different road profiles: (a) different content of Crumb Rubber (CR), (b) different visual road deterioration.

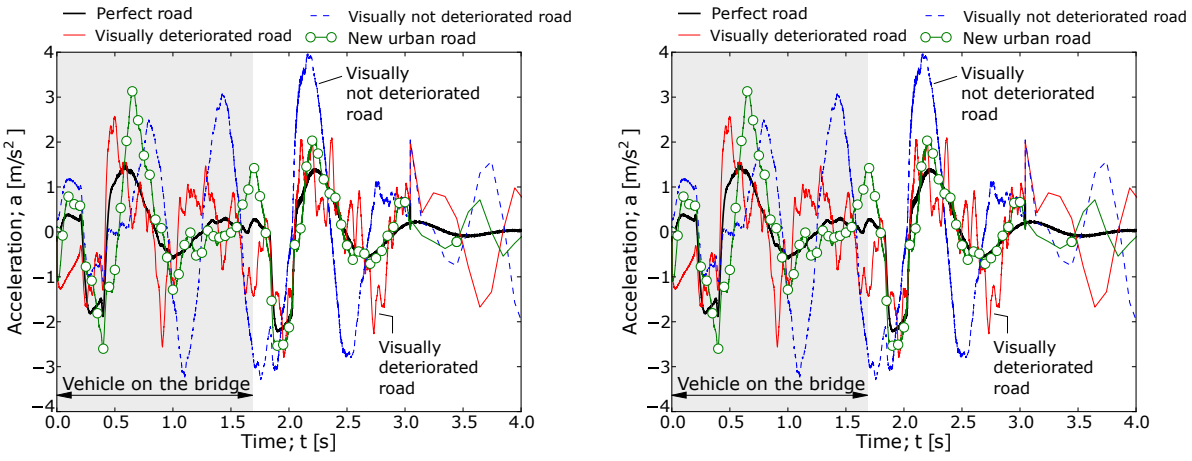

FIG. 9. Time-history of the acceleration in the vehicle cabin for different pavements: (a) sample #1, (b) sample #2.

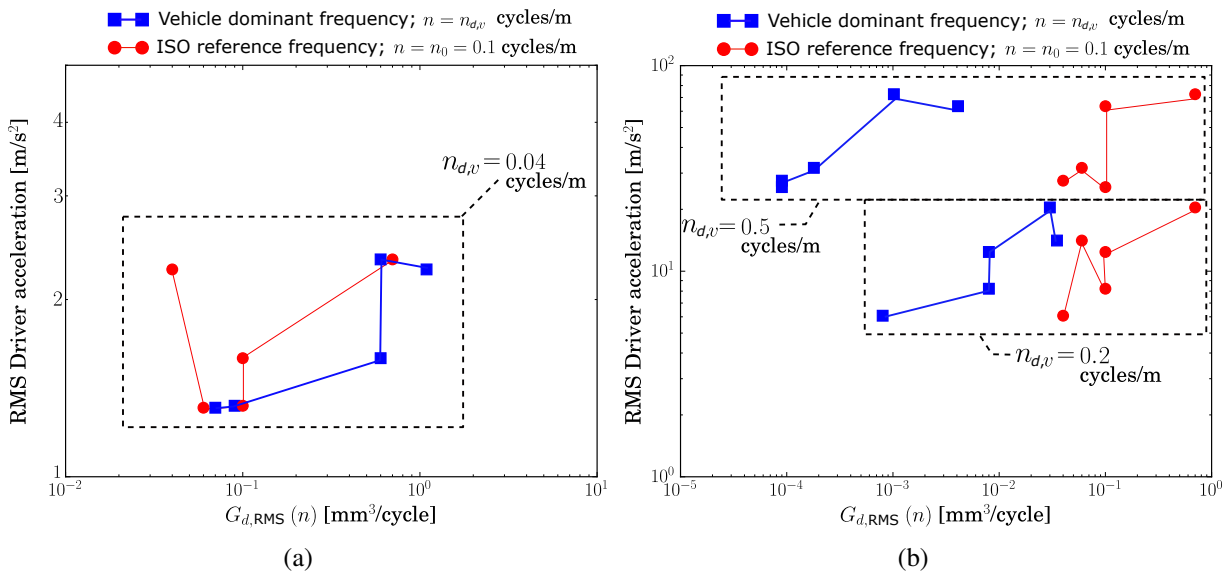

FIG. 10. Peak RMS acceleration in the vehicle versus the PSD acceleration evaluated at different frequencies: (a) original AASHTO vehicle, $f_{d,v} = 1$ Hz ($n_{d,v} = 0.04$ cycles/m), (b) modified vehicles with $f_{d,v} = 5$ and 12.5 Hz ($n_{d,v} = 0.2$ and 0.5 cycles/m, respectively). Arithmetic mean of the sets of 10 profiles generated from the measured road pavements.